Absolute differential bremsstrahlung cross sections for 0.4–2-keV electrons scattered by Ar, Kr, and Xe atoms

E. V. Gnatchenko, A. N. Nechay, and A. A. Tkachenko

B. Verkin Institute for Low Temperature Physics and Engineering of the National Academy of Sciences of Ukraine, 47 Lenin Avenue, Kharkiv 61103, Ukraine

The dependences of absolute differential bremsstrahlung cross sections on 0.4–2-keV electron scattering by supersonic gas jets of Ar, Kr, and Xe versus electron energy as well as the atom number Z were studied experimentally. The bremsstrahlung photons have been detected at an angle 97° to the incident electron beam in the ultrasoft x-ray spectral region 70–200 eV. It is found that as the electron energy is increased from 0.4 to 2 keV, the absolute bremsstrahlung cross section for Xe increases throughout the whole electron energy range and the energy dependencies of cross sections for Ar and Kr displayed maxima at electron energies of ∼0.7 keV (Ar) and ∼1 keV (Kr). These experimental results cannot be explained in the framework of Bethe and Heitler and Sauter theory, based on the first Born approximation. The experimental absolute differential bremsstrahlung cross sections for Ar, Kr, and Xe are considerably larger then the tabulated values of ordinary bremsstrahlung. The obtained Z dependence of bremsstrahlung cross section differs with calculated one, particularly for large atomic number Z.

PACS number(s): 34.80.−i, 78.70.−g

I. INTRODUCTION

In recent years, atomic gas targets have been widely used in detailed studies of the elementary processes of photon radiation occurring in collisions of a charged particle with an atom. The gas targets made it possible to observe a two-photon process of bremsstrahlung (BS) [1] and measure absolute cross sections of high-energy electron ($E > 25$ keV) BS from Ne, Ar, Kr, and Xe atoms [2]. Experiments in which an electron-beam-excited supersonic jet evacuating into vacuum is used as a dense gas target are of special interest for these studies [3,4]. Thanks to the formation of a jet with a large Mach number ($M \approx 10$) and the low temperature of the gas in the jet (around 70 K), due to its isentropic expansion into vacuum, the velocity of directed motion of the particles of the jet in the axial direction is much greater than the radial velocities of the random thermal motion. As a result, a dense gas jet-target with sharp boundaries with the vacuum is obtained in the vacuum chamber, making it possible to study subtle effects on the interaction of the electron beam with the particles of the jet target. One of the advantages of the gas-jet method is a possibility of placing the electron gun near the jet in order to enable the study of radiation spectra emerging as the electron beam consecutively probes the electron shells of the atom from the valence to the innermost K shell. By varying the electron energy, it is possible to create favorable conditions for the study of BS spectra without superimposing on them the characteristic emission lines of atoms.

It is this gas-jet technique that has led to considerable progress in the bremsstrahlung physics as a result of the observation of polarization bremsstrahlung (PBS) [5–7].

Bremsstrahlung, which arises in the scattering of a charged particle by a target particle (an atom or ion), is formed by two mechanisms. In the first case the photons are emitted by the incoming charged particle as it is braked in the static field of the target particle; this is ordinary brems-

strahlung (OBS). OBS is characterized by a smooth spectral distribution of the photons and is well described by the theory of Bethe and Heitler [8] and Sauter [9] (BHS), which is based on a screening approximation. According to that approximation, the electron shell of the atom or ion is replaced by the electrostatic field that it creates.

The essence of the second mechanism [10] is as follows. The photons of the continuum are emitted not by the scattered particle, as in the first mechanism, but by the electrons of the target particle due to its dynamic polarization by the field of the incoming particle. The bremsstrahlung formed by this mechanism has been given the name PBS. Unlike the process described by the BHS theory, the electrons of the target are now treated as a dynamical system having internal degrees of freedom. Theoretical studies [10] have established that in this case taking the influence of the electron shell of the atoms or ions into account will in a number of cases lead to substantially different results. The difference lies in different frequency and angular characteristics of the radiation and also in the radiation probability that is independent of the mass of the incoming particle.

Experimentally, PBS was first observed in the ultrasoft x-ray region of photon energies 70–220 eV in the scattering of 0.6-keV electrons on Xe atoms [5]. The PBS was manifested as a wide band with a structure close to that of the "giant" resonance in the photoabsorption spectrum of Xe atoms. Later, the PBS spectrum profile [6] and intensity dependence on electron energy (0.3–0.9 keV) [11] were studied. The spectral distribution of the absolute differential cross section for total bremsstrahlung, including the ordinary and polarization components, on the scattering of 0.6-keV electrons by free xenon atoms was also measured [7].

One of the most important aspects of the experimental study of the BS from electron scattering on atoms is verification of the BHS theory, which takes into account the screening of the nucleus by the atomic electrons. The experiments made up to now, limited mainly to electrons of rela-
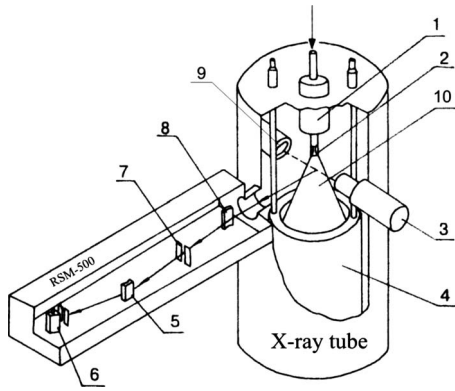
FIG. 1. Schematic view of the experimental setup: 1, heat exchanger; 2, supersonic conic nozzle; 3, electron gun; 4, cryogenic pump; 5, diffraction grating; 6, proportional counter; 7, entrance slit of the spectrometer-monochromator; 8, mirror; 9, Faraday cup; 10, supersonic gas jet.

tively high energies [12,13], show no substantial deviation from the BHS theory.

However, our recent ultrasoft x-ray experimental study of ordinary BS from 0.4–2-keV electrons scattered by Ar and Kr atoms has shown an increase in ordinary BS cross section with growing electron bombarding energy up to a pronounced maximum, which is followed then by a cross section decrease [14,15]. This result is in obvious contradiction with the BHS theory, according to which cross section of ordinary BS originating in the scattering of a nonrelativistic electron by an atom decreases as electron energy grows.

It should be noted that the cross sections reported in the above papers are in relative units which makes it more difficult to compare the experimental results with the theory.

To continue the BS studies initiated in Refs. [14,15], this paper has for an object to study the dependences of absolute BS cross sections on energy of electrons scattered by Ar, Kr, and Xe atoms.

II. EXPERIMENT

The experimental setup used to study bremsstrahlung is shown in Fig. 1. It consists of an x-ray tube with a supersonic gas jet as the anode and an RSM-500 spectrometer-monochromator. The working principle of the setup is as follows. The gas to be investigated issues out of a high-pressure vessel to the heat exchanger 1 and then is formed by a supersonic conical nozzle 2 into a jet 10 flowing into the vacuum chamber. The diameter of the nozzle throat is 0.3 mm. The area ratio of the exit section and the throat is 59.3, the cone angle is 9.5°. The gas brought by the jet is pumped out with a cryogenic liquid-hydrogen cooled pump 4. Owing to the distinct boundaries between the supersonic gas flow and the vacuum (10^{-2} Pa), the electron gun 3 is placed only 40 mm from the jet. The electron gun is a two-electrode Pierce gun with a LaB_6 cathode. By choosing the proper shape of the gun electrodes, the electric field is configured in such a way that it focuses electrons emitted from all over the cathode into a parallel beam. A magnetic lens having 500 turns of MGTF 0.07 wire is used to additionally focus the
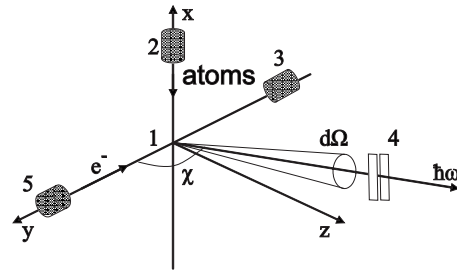

FIG. 2. Geometric scheme of the experiment: 1, collision region; 2, supersonic nozzle; 3, Faraday cup; 4, separating diaphragm; 5, electron gun; χ, angle between the motion directions of electrons and analyzed photons; $d\Omega$, solid angle of radiation collection.

electron beam. A water-cooled copper shield is used for thermal decoupling between the heated elements of the gun and the magnetic lens to avoid overheating of the lens. Depending on electron energy, the current flowing through the lens is varied in the range from 0.2 to 0.8 A, the beam diameter not exceeding 2 mm. The electron-beam current is measured with a copper Faraday cup (9). The Faraday cup's length is five times its diameter, its bottom is cone shaped with an opening angle of 90°. The Faraday cup is cooled by running water. Such a construction makes it possible to suppress the background x-ray radiation arising when the electron beam hits the cup. To eliminate the influence of secondary electrons on the measured current, the Faraday cup is given a positive potential of +50 V. The energy of electrons was varied from 0.4 to 2 keV, the current of electrons being maintained constant at 20 mA for the various electron energies. The current density was a function of electron energy and varied from 0.32 to 1.2 A/cm^2 due to the variation in electron-beam diameter from 1 to 2 mm as a result of the beam focusing in the region of jet excitation. The methodical study of BS performed in Ref. [16] has demonstrated however that BS intensity remains constant within the measurement error of 10% upon those variations. The electron beam crossed the rare gas jet at a distance of 10 mm from the nozzle exit section. The generated radiation is focused by a spherical mirror 8 onto the entrance slit 7 of the RSM-500 spectrometer-monochromator and is then dispersed into a spectrum by a gold-coated diffraction grating 5 having 600 lines/mm. Beyond the exit slit of the RSM-500 spectrometer-monochromator the radiation is registered with a proportional counter 6 filled with methane to a pressure of 1.5 $\times 10^4$ Pa. The window on the counter is made of nitrocellulose. A description of the apparatus is given in Refs. [6,17]. The experiments were carried out in the regime of single collisions evidenced by the linear dependence of BS intensity on electron current density.

In the studies reported here, we measured differential spectra of BS. The geometry of the experiment is shown in Fig. 2. The jet of rare gas atoms formed by the supersonic nozzle 2 is crossed by an electron beam; the radiation arising in the place of their intersection goes to the separating diaphragm 4. The angle between the directions of the incident electrons and the analyzed photons is $\chi=97°$. The solid angle of radiation collection is $d\Omega=1.7\times10^{-3}$ sr. The angle is defined as $d\Omega=S/R^2$, where S is the area of the separating

diaphragm (0.3 cm^2) and R is the distance between the jet axis and the separating diaphragm (13.3 cm). Error in determination solid angle is 10%.

The experiments were performed under the following conditions:

(1) The spectral range under investigation was 6–18 nm.

(2) The spectral resolution was 1 Å.

(3) The electron energy was varied in the range 0.4–2 keV.

(4) Our measurements have shown that the current registered in the Faraday cup after electrons have passed through the gas target differs little from that of electrons that hit the target. The error in determination of electron density n_e does not exceed 10%.

(5) The gas pressure and temperature at the nozzle entrance were $P_0=6\times10^4$ Pa and $T_0=300$ K, respectively. The density of Ar, Kr, and Xe atoms in the collision region under the chosen experimental conditions was $n_a=5 \times 10^{15}$ at/cm^3. The error in determining the density of atoms did not exceed 10%. For a monoatomic supersonic gas jet flowing through a nozzle with known geometrical parameters (pressure and temperature of gas being kept constant at the nozzle entrance), the density profile in the place of intersection of the jet and the electron beam is very weakly dependent on mass number of the element. This is due to the fact that gas density in the exit cross section of nozzle only depends on gas density at the nozzle entrance as well as on ratio of gas flux velocities in the exit and critical cross sections of nozzle and the ratio of heat capacities $\gamma=c_p/c_v$ [18]. The ratio of the velocities and the jet opening angle are determined by the nozzle parameters and the ratio of heat capacities, the latter may be considered constant since the value $\gamma=c_p/c_v$ varies not more than by 1% for Ar, Kr, and Xe [19]. The BS self-absorption did not exceed 5%.

(6) The volume of the excitation region was $A \approx 0.1$ cm^3. The x-ray tube allows visual viewing of the supersonic jet excited by an electron beam (through an observation window) so the dimensions of the excitation region were determined visually by means of a transparent calibration grid with 0.5-mm-long square cells. Error in determination of the region excitation is 10%.

III. METHOD FOR OBTAINING ABSOLUTE DIFFERENTIAL BREMSSTRAHLUNG CROSS SECTIONS

The spectral distribution of the absolute differential cross section for bremsstrahlung is defined as

$$\frac{d^2\sigma^{BS}}{d\omega d\Omega} = \frac{I^{BS}(\hbar\omega)}{n_a n_e v \hbar\omega} \frac{1}{A}, \tag{1}$$

where $I^{BS}(\hbar\omega)$ (erg/s eV) is the BS intensity at the photon energy $\hbar\omega$ (eV) in solid angle $d\Omega$; n_a and n_e (cm^{-3}) are the densities of atoms and electrons, respectively; v (cm/s) is the electron velocity; and A (cm^3) is the excitation region volume.

In order to determine the absolute bremsstrahlung intensity $I^{BS}(\hbar\omega)$, the spectral dependence of the absolute sensitivity of the x-ray spectral equipment is determined by the following procedure [7,20].

The spectral distribution of the intensity of total bremsstrahlung in the solid angle $d\Omega$ from the scattering of electrons from atoms can be expressed as

$$I^{BS}(\lambda) = \frac{k(\lambda)N_{\Delta\lambda}\hbar\omega}{\Delta\lambda}. \tag{2}$$

Here, $k(\lambda)$ (photon/count) is the spectral distribution of the absolute sensitivity of the RSM-500 x-ray spectrometer, $N_{\Delta\lambda}$ is the signal at the output of the spectrometer that is detected in the bremsstrahlung spectral range $\Delta\lambda$ (count/s), and $\hbar\omega$ (erg) is the average photon energy in the spectral range $\Delta\lambda$ (nm).

In turn, the spectral distribution of the absolute sensitivity, $k(\lambda)$, is described by the expression

$$k(\lambda) = \frac{Q(\lambda)d\lambda d\Omega}{N_{\Delta\lambda}}. \tag{3}$$

Here, $Q(\lambda)$ (photon/s nm sr) is the radiation flux density of a calibrated source with a known spectral distribution of intensity incident on the entrance slit of the spectrometer.

A supersonic argon jet excited by an electron beam was used as a calibrated radiation source. The spectral distribution of the radiation flux flow, $Q(\lambda)$, is determined as follows. The total radiation flux Q (photon/s sr) in a wavelength range of 5–170 nm is measured by an SXUV-100 detector with a known spectral sensitivity in absolute units. Simultaneously with the measurement of the integral radiation flux, the relative distributions of the intensities $I_1(\lambda)$ and $I_2(\lambda)$ in the radiation spectral ranges 5–55 nm and 50–170 nm of the argon jet, respectively, are detected by the RSM-500 spectrometer and SP-68 vacuum monochromator. The spectra obtained are corrected to the efficiency of the corresponding measuring instruments. The relative intensity distribution $I(\lambda)$ in the entire wavelength range 5–170 nm is determined as follows:

$$I(\lambda) = I_1(\lambda)\frac{S_2}{S_1} + I_2(\lambda), \tag{4}$$

where S_1 and S_2 are the areas of the spectral section 50–55 nm that are detected by the RSM-500 and SP-68 instruments, respectively. After the determination of Q and $I(\lambda)$, the spectral distribution of the radiation flux density, $Q(\lambda)$, of the supersonic argon jet in the entire wavelength range is determined as

$$Q(\lambda) = \frac{QI(\lambda)}{\int_5^{170}I(\lambda)d\lambda}, \tag{5}$$

where the integral is the area of the spectrum in a range of 5–170 nm.

Figure 3 shows the spectral distribution $k(\lambda)$ of the absolute sensitivity of the RSM-500 spectrometer obtained by the above procedure. The error in the determination of the absolute differential BS cross section was no more than 40%.

IV. RESULTS AND DISCUSSION

Figure 4 shows the experimental differential BS spectra in the wavelength range of 6–18 nm (photon energy region 70–
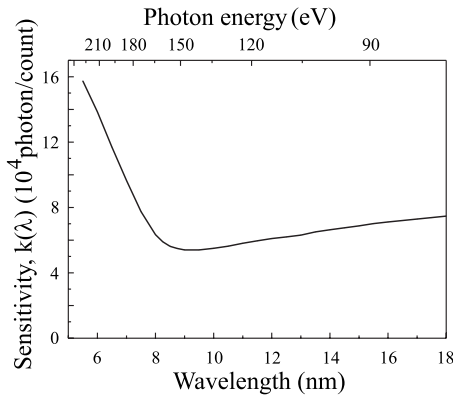
FIG. 3. Spectral distribution of the absolute sensitivity of the RSM-500 monochromator in a wavelength range of 6–18 nm. The error in the determination of the absolute sensitivity is no more 30%.

200 eV) obtained in the scattering of 0.6-keV electrons by Ar, Kr, and Xe atoms.

The BS spectra for Ar and Kr are characterized by a smoothly distributed intensity which is inversely proportional to the wavelength squared (see the inset in Fig. 4), i.e., its behavior coincides with that of the BS intensity in the case of a thin target [21]. The same spectral behavior of BS is also observed for electrons with other energies from the 0.4–2-keV range. This is indicative of the fact that when electrons of intermediate energies (0.4–2 keV) are scattered by Ar and Kr atoms, the bremsstrahlung in the wavelength range of 6–18 nm is formed as a result of their deceleration in the static field of the atoms. The contribution of polarization BS resulting from dynamical polarization of the atom by the field of the incident electron turns out to be very small in this case.

The BS spectrum on the scattering of electrons by Xe atoms differs appreciably from the BS spectra for Ar and Kr. Instead of the smooth spectral distribution of intensity decreasing as $1/\lambda^2$ (the dashed line in Fig. 4), we observe a broad intensity maximum originating from polarization bremsstrahlung formed by virtual excitations of Xe atoms into the continuous spectrum above the $4d$ ionization thresh-
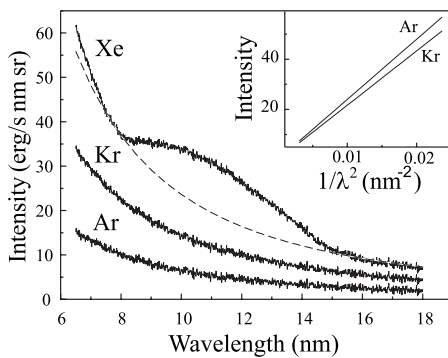

FIG. 4. Absolute differential spectra of total BS for 0.6-keV electrons scattered on Ar, Kr, and Xe atoms. The dashed line is the spectral dependence of ordinary BS intensity. The inset shows the BS spectra as functions of $1/\lambda^2$ for Ar and Kr in the wavelength range 6–18 nm.
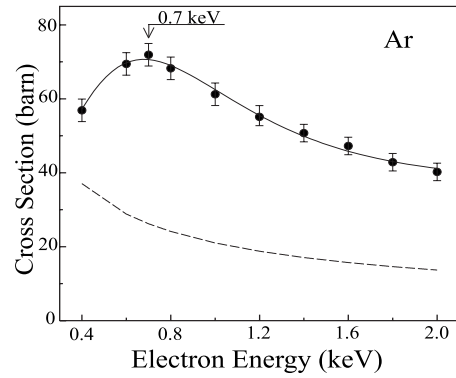

FIG. 5. Absolute differential BS cross section versus energy of electrons scattered by Ar atoms. The solid circles are experimental data at the photon energy $\hbar\omega = 177$ eV. The dashed curve is calculation on the basis of the data by Pratt *et al.* [24] for the photon energy $\hbar\omega = 200$ eV. The errors shown are statistical.

old. As can be seen in Fig. 4, in the spectral regions $\lambda > 15$ nm and $\lambda < 8$ nm, where the PBS contribution is small, the wavelength dependence of BS intensity is practically the same as that of the intensity of ordinary BS in the case of a thin target [21]. In the range of 8–14.5 nm, such a behavior breaks down due to the PBS contribution which is superimposed on the spectrum of ordinary BS as an emission band peaked at ~10 nm.

To study dependences of absolute differential BS cross section on electron energy we chose the wavelength interval of 6–8 nm (photon energy ranging from 155 to 200 eV). The reason is that a number of characteristic emission lines of Ar, Kr, and Xe atoms are superimposed on BS spectra in the wavelength region over 8 nm as electron energy increases from 0.4 to 2 keV [22,23]. The spectra in the chosen wavelength range are formed only in the process of ordinary BS for all the electron energies studied.

Figures 5–7 show the experimental dependences of isochromatic absolute differential BS cross sections on energy of electrons scattered by Ar, Kr, and Xe atoms at the photon energy 177 eV (Ar, Xe) and 165 eV (Kr).
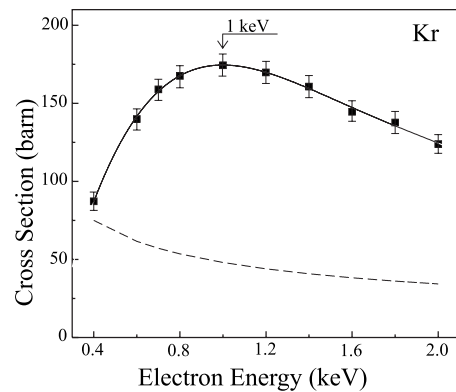

FIG. 6. Absolute differential BS cross section versus energy of electrons scattered on Kr atoms. The solid circles are experimental data at the photon energy $\hbar\omega = 165$ eV. The dashed curve is calculation on the basis of the data by Pratt *et al.* [24] for the photon energy $\hbar\omega = 200$ eV. The errors shown are statistical.
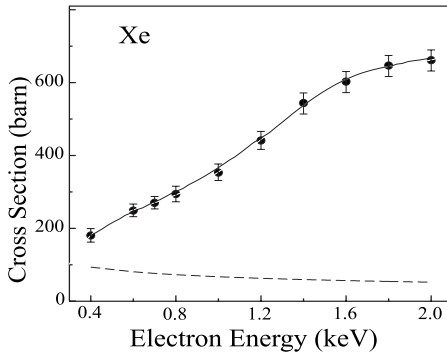
FIG. 7. Absolute differential BS cross section versus energy of electrons scattered on Xe atoms. The solid circles are experimental data at the photon energy $\hbar\omega = 177$ eV. The dashed curve is calculation on the basis of the data by Pratt *et al.* [24] for the photon energy $\hbar\omega = 200$ eV. The errors shown are statistical.

Analysis of the results obtained make it possible to find some common features characterizing the changes in the differential BS cross section that occur as electron energy changes. All the observed isochromatic curves differ noticeably from the dependence of BS cross section on electron energy predicted by the BHS theory. According to the theory, the cross section of BS should decrease with increasing electron energy in the process of scattering of a nonrelativistic electron by an atom [8,9]. However, in the case of Ar (Fig. 5) there is an increase in BS cross section up to a pronounced maximum with electron energy growing from 0.4 to 0.7 keV which is followed then by a BS cross section decrease as electron energy keeps growing from 0.8 to 2 keV. For Kr, the BS cross section dependence (Fig. 6) is generally the same as that for Ar, except for the energy position of the maximum: $E_{max}(\text{Ar}) \sim 0.7$ keV and $E_{max}(\text{Kr}) \sim 1$ keV. In order to explain the experimentally observed behavior of the dependences of relative BS cross section on energy of electrons scattered by Ar and Kr atoms, a new phenomenological modification of the quasiclassical approximation, also known as *soft photon approximation* (SPA) [25], was employed in Ref. [15] to calculate the BS cross sections using the data on elastic electron-scattering cross section. A qualitative agreement between the calculated and experimental results has been obtained.

As for the case of Xe (Fig. 7), an increase in cross section of ordinary BS is observed throughout the whole electron energy range studied. As energy grows over 1.6 keV, the increase in BS slows down.

To compare our experimentally obtained values of differential cross section with theoretical results, we used the numerical calculations of ordinary BS energy spectra taken from Ref. [24]. In those calculations, the electron bremsstrahlung process was described as a single-electron transition in a relativistic self-consistent screened potential. The energy spectra of BS were calculated for neutral atoms (with atomic numbers $2 \le Z \le 92$) over the whole solid angle and for incident electrons having the energy $E \ge 1$ keV for the following ratios: $\hbar\omega/E = 0.0, 0.1, 0.2, \ldots, 1.0$. To calculate the cross sections for the electron energies $E \le 1$ keV, we extrapolated the table data from Ref. [24] for $E = 1, 2.5$, and

TABLE I. Comparison of the experimental and theoretical [24] cross sections of BS for 1-keV electrons scattered on Ar, Kr, and Xe atoms at the photon energy $\hbar\omega = 200$ eV.

| Element | Z | Cross section (b/sr) | | $d\sigma^{\text{expt}}/d\sigma^{\text{theory}}$ |
		Experiment	Theory	
Ar	18	61	21	2.9
Kr	36	175	48	3.7
Xe	54	270	67	4.0

5 keV down to $E = 0.4$ keV for the ratios $\hbar\omega/E = 0.1$ and 0.2. Figures 5–7 show the calculated BS cross section curves normalized to unit solid angle (without taking into account the BS anisotropy) for Ar, Kr, and Xe. Table I shows the obtained experimental and calculated cross sections for Ar, Kr, and Xe at an electron energy of 1.0 keV. The following conclusions can be drawn from Table I and Figs. 5–7:

(i) The magnitude of the experimentally obtained BS cross sections is some three times larger than its calculated value for Ar and four times larger for Kr and Xe at the electron energy of 1 keV (see Table I).

(ii) The isochromatic curves of the experimental differential cross section for Ar, Kr, and Xe differ strongly from the calculated data in the whole electron energy range studied 0.4–2 keV. However, in the case of Ar and Kr the experimental curves of BS cross section behaves similarly to the calculated one for electron energies growing from 1 to 2 keV (Figs. 5 and 6), the absolute experimental values being considerably larger than the calculated ones.

(iii) The experimental differential BS cross section for Xe increases throughout the whole range of electron energy and exceeds that of the calculated one by a factor 8 for $E = 2$ keV (see Fig. 7).

As can be seen from Figs. 5–7, the BS cross sections and their behavior with electron energy depend on charge Z of the atomic nucleus. As Z grows, the absolute values of BS cross section grow as well, while the maximum of the BS cross section for Kr shifts toward greater electron energies with respect to its position for Ar or is altogether absent in the case of Xe.

Figure 8 shows the theoretical dependence of total BS cross section on atomic number calculated using the data taken from Ref. [24] for the electron energy $E = 2.5$ keV and photon energy $\hbar\omega = 200$ eV, which are close to our experimental values. Figure 8 also shows the differential BS cross sections for Ar, Kr, and Xe obtained in this work, the measured cross section for Ar (atomic number $Z = 18$) is superposed with the theoretical one, the cross sections for Kr and Xe are normalized to that for Ar. The BS cross section for Kr coincides the calculated curve within the experimental error, but in the case of Xe, as can be seen from Fig. 8, there is a noticeable difference between the curves. As it has already been noted above, the spectrum of BS arising in the scattering of electrons by Xe atoms in the photon energy range 70–200 eV (see Fig. 4) consists of ordinary and polarization BS spectra. In Ref. [10] it was demonstrated that the PBS results in descreening of the nucleus. The theoretical curve in Fig. 8 was obtained by using the results of numerical calcu-
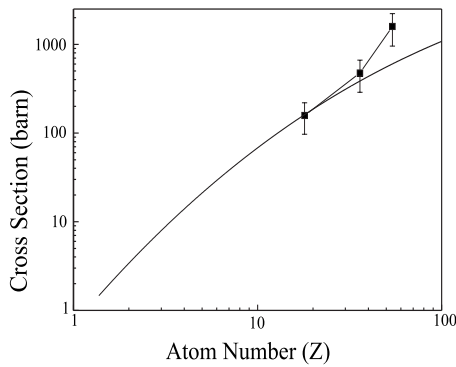
FIG. 8. BS cross section as a function of nucleus number Z at the photon energy $\hbar\omega=200$ eV. The calculated curve (Pratt *et al.* [24]) for the electron energy $E=2.5$ keV is the solid line. The data measured at the electron energy $E=2.0$ keV are solid squares.

lations of ordinary BS energy spectrum performed in the screening approximation, i.e., without taking into consideration the descreening effect. Therefore, the discrepancy between the experimental and theoretical curves observed for Xe is likely to be due to the descreening of the nucleus by the atom shell electrons.

V. CONCLUSIONS

The paper reports for the first time absolute differential cross sections for bremsstrahlung on scattering of 0.4–2-keV electrons by free atoms of rare gases in the photon energy range 70–200 eV. The observed dependences of BS cross section on electron energy differ considerably from those predicted by the BHS theory based on the Born approximation. Instead of the expected decrease in BS cross section

with growing electron energy for Ar and Kr, there is an increase in it up to a pronounced maximum which is then followed by a decrease. For electrons scattered by Xe atoms, the BS cross section increases with electron energy growing from 0.4 to 2 keV. Comparison of the experimental absolute differential BS cross sections with the theoretical ones shows that the absolute values of the experimental cross sections are several times those calculated. In the case of Ar and Kr, the experimental isochromatic BS cross-section curves measured in the electron energy range 1–2 keV are close to the calculated ones. However for Xe, the curves are different throughout the whole energy range studied. The obtained experimental absolute BS cross sections and their behavior with electron energy depend on nucleus charge, Z. Thus the obtained experimental results demonstrate that the BHS theory cannot be applied to describe the process of BS formation on the scattering of intermediate-energy electrons (0.4–2 keV) by Ar, Kr, and Xe atoms.

To have a more comprehensive description of the process of BS formation in the scattering of intermediate-energy electrons by free rare-gas atoms we believe that some experimental study of BS in wider electron energy and atomic number ranges is needed. Calculations of BS cross sections in the ultrasoft x-ray energy region for various angles between the direction of the moving electrons and that of the outgoing BS photons should also be made in the case of intermediate-energy electrons in a wide range of atomic numbers.

ACKNOWLEDGMENTS

[1] R. Hippler, Phys. Rev. Lett. **66**, 2197 (1991).

[2] S. Portillo and C. A. Quarles, Phys. Rev. Lett. **91**, 173201 (2003).

[3] P. S. Pogrebnjak, Yu. A. Pavlenko, E. T. Verkhovtseva, Ya. M. Fogel, and V. F. Udovenko, Prib. Tekh. Eksp. **5**, 193 (1974).

[4] E. T. Verkhovtseva, E. A. Katrunova, A. E. Ovechkin, and Ya. M. Fogel, Chem. Phys. Lett. **50**, 463 (1977).

[5] E. T. Verkhovtseva, E. V. Gnatchenko, and P. S. Pogrebnjak, J. Phys. B **16**, L613 (1983).

[6] E. T. Verkhovtseva, E. V. Gnatchenko, B. A. Zon, A. A. Nekipelov, and A. A. Tkachenko, Zh. Eksp. Teor. Fiz. **98**, 797 (1990); Sov. Phys. JETP **71**, 443 (1990).

[7] E. V. Gnatchenko, A. A. Tkachenko, and A. N. Nechay, Pis'ma Zh. Eksp. Teor. Fiz. **86**, 344 (2007); JETP Lett. **86**, 292 (2007).

[8] H. Bethe and W. Heitler, Proc. R. Soc. London, Ser. A **146**, 83 (1934).

[9] F. Sauter, Ann. Phys. **401**, 217 (1931).

[10] *Polarization Bremsstrachlung of Particles and Atoms*, edited by V. N. Tsytovich and I. M. Oiringel (Plenum Press, New York, 1992).

[11] E. T. Verkhovtseva and E. V. Gnatchenko, Low Temp. Phys. **28**, 270 (2002).

[12] R. Hippler, K. Saeed, I. McGregor, and H. Kleinpoppen, Phys. Rev. Lett. **46**, 1622 (1981).

[13] M. Semaan and C. Quarles, Phys. Rev. A **24**, 2280 (1981); **26**, 3152 (1982).

[14] E. V. Gnatchenko, A. A. Tkachenko, and E. T. Verkhovtseva, Surf. Rev. Lett. **9**, 651 (2002).

[15] E. V. Gnatchenko, A. A. Tkachenko, E. T. Verkhovtseva, and B. A. Zon, Phys. Rev. Lett. **95**, 023002 (2005).

[16] A. A. Tkachenko, E. V. Gnatchenko, and E. T. Verkhovtseva, Opt. Spectrosc. **78**, 208 (1995).

[17] E. T. Verkhovtseva, E. V. Gnatchenko, A. A. Tkachenko, and B. A. Zon, Radiat. Phys. Chem. **74**, 51 (2005).

[18] L. D. Landay, E. M. Lifshitz, *Mechanics Sploshnych Sred* (Izd. Tech.-Teor. Literature, Moskow, 1973).

[19] G. W. Kaye and T. H. Laby, *Tables of Physical and Chemical Constants* (Longmans, Green and Co., London, 1958).

[20] A. A. Tkachenko, E. V. Gnatchenko, and E. T. Verkhovtseva, Zh. Tekh. Fiz. **64**, 136 (1994).

[21] T. J. Peterson, Jr. and D. A. Tomboulian, Phys. Rev. **125**, 235

(1962).

[22] E. T. Verkhovtseva, Izv. Akad. Nauk SSSR, Ser. Fiz. **48**, 675 (1984).

[23] E. T. Verkhovtseva, E. V. Gnatchenko, P. S. Pogrebnjak, and A. A. Tkachenko, J. Phys. B **19**, 2089 (1986).

[24] R. H. Pratt, H. K. Tseng, C. M. Lee, L. Kissel, C. McCallum, M. Riley, At. Data Nucl. Data Tables **20**, 175 (1977); **26**, 477 (1981).

[25] J. M. Jauch and F. Rorlich, Helv. Phys. Acta **27**, 613 (1954).